

MEMBRANE SUPPORTED CPW-FED WIDEBAND SLOT ANTENNA FOR MILLIMETER WAVE APPLICATIONS

S. Krishnan^{1,*}, J. Boone¹, H. La Rosa², and S. Bhansali³

¹Clean Energy Research Center, College of Engineering, University of South Florida, Tampa, FL 33620, USA

²Texas Instruments, Clearwater, FL 33759, USA

³Department of Electrical and Computer Engineering, College of Engineering, Florida International University, Miami, FL 33174, USA

Abstract—A low profile CPW fed millimeter wave rectangular slot antenna operating with a wideband; centered at 94 GHz has been designed, fabricated and tested on a 10 μm silicon diaphragm. To improve the bandwidth of the conventional slot antenna a C-shaped tuning stub has been incorporated. Measurement results show that the antenna operates from 75 to 105 GHz with a reflection coefficient better than -10 dB. At its resonant frequency the fabricated slot antennas have a reflection co-efficient ranging from -25 dB to -35 dB. The bandwidth of the antenna with a tuning stub was found to be over 30% at -10 dB. By using the slot antenna with a C-shaped tuning stub the bandwidth has been shown to improve, which could be used for several Millimeter wave applications.

1. INTRODUCTION

Interest in millimeter wave devices consisting of planar antennas have increased dramatically due to its shorter wavelength characteristics, which enables reduction in the component size and cost of the overall system. This allows for the production of compact systems for passive millimeter wave imaging, remote sensing, radio astronomy, cloud radar, automotive collision warning, and adaptive cruise control systems [1–8]. These applications require antenna systems operating at millimeter wave to have high gain, low side lobes and wide bandwidths. At millimeter-wave frequencies, the antenna design and performance are

Received 21 November 2011, Accepted 1 March 2012, Scheduled 14 March 2012

* Corresponding author: Subramanian Krishnan (skrishn4@usf.edu).

usually based on the high dielectric constant of the substrate [9]. However, the high permittivity of the substrate gives rise to surface waves, potentially increasing the side lobe levels and reducing the radiation efficiency. To minimize this effect, the thickness of the substrate has to be reduced.

In recent years, the micromachining technology has been proposed for the fabrication of millimeter wave devices on silicon membranes [10]. By realizing these devices on thin membranes, the effect of surface waves can be minimized. Furthermore, unwanted propagation can also be suppressed, which could otherwise introduce additional losses [11]. Many researchers have presented different types of CPW-fed slot antennas for millimeter wave applications [12–17]. However, the bandwidth of a conventional slot antenna is not wide enough to cover the interested spectrum of millimeter wave. In this paper, we present the design, fabrication and testing of a rectangular slot antenna with tuning stub supported by a 10 μm silicon membrane. The tuning stub integrated in the slot antenna improves its bandwidth performance. The antenna design with a tuning stub along with a CPW transition is discussed in Section 2. The fabrication of the antenna is presented in Section 3. Finally Section 4 discusses the measurement techniques and the characteristics of the millimeter wave antenna.

2. ANTENNA AND TUNING STUB DESIGN

2.1. Antenna

In this section, the design of the membrane supported antenna with tuning stub, fed with a CPW configuration is presented. Figure 1 shows the configuration of the millimeter wave slot antenna with a tuning stub. Slot antennas have also been designed in the past using a microstrip feeding mechanism [18]. The design has been performed using Agilent’s Momentum Electromagnetic Simulator, which predicts the performance of the membrane-supported antenna in terms of radiation pattern, antenna efficiency and input impedance.

A high-resistivity silicon substrate was used for this design since it can be easily integrated with standard fabrication technologies. The silicon substrate permittivity was 11.7 with a loss tangent of 0.0008. The antenna was designed with a CPW feed line. In order to achieve proper radiation at such high frequencies, the thickness of the substrate was reduced from 250 μm to 10 μm . This reduction helped eliminate the propagation of surface waves that can appear in substrates at extremely high frequencies. Designing the antenna on a thicker substrate would have yielded poor radiation caused by wave disruption. Since the thickness of the substrate was altered,

the line width has to be changed accordingly to match the antenna impedance. The slot antenna was then scaled via dimensions to achieve a $50\ \Omega$ impedance match at the center frequency. Next, the tuning stub was integrated in the slot and designed to increase the antenna bandwidth to achieve maximum performance. The CPW lines were then designed at $50\ \Omega$ impedance in order to integrate with the antenna. The design specifications of CPW transition are discussed in detailed in the following section. The ground plane of the antenna was designed to be $1.25\lambda_{eff}$ long and $0.9\lambda_{eff}$ wide. At 94 GHz on a silicon substrate, these dimensions are equivalent to $1.57\ \text{mm} \times 1.1\ \text{mm}$. As shown in the Fig. 1(a) the slot is opened $0.26\ \text{mm} \times 0.3\ \text{mm}$ inside the ground plane. The size of the slot is $1.05\ \text{mm} \times 0.5\ \text{mm}$. These dimensions have an effect on the resonant frequency of the antenna. By altering its width and length, the center frequency will begin to shift. Typically, further opening the slot increases the center frequency, whereas closing the slot more decreases the center frequency as shown in Table 1. This is due to the fact that suppressing the radiation of the slot causes the resonance to shift toward higher frequencies, while a wider radiating slot creates a lower frequency shift. However, these adjustments are design sensitive and will affect each antenna's behavior differently.

2.2. Tuning Stub Design

Figure 1(b) illustrates the geometry and dimension of the tuning stub used in this antenna. Several types of tuning stubs have been designed based on the bandwidth and operating frequency [19]. A C-

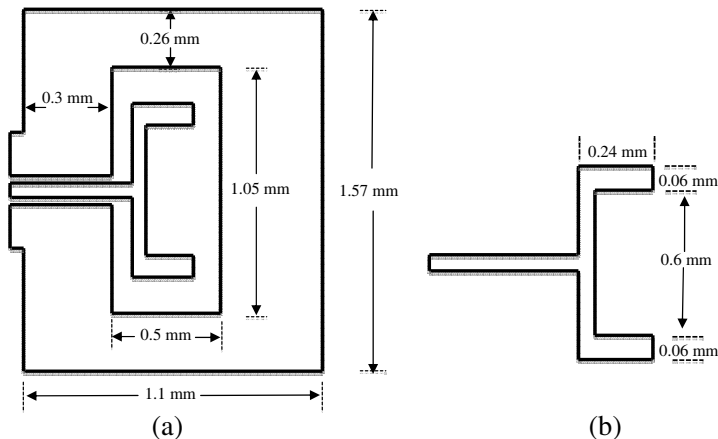


Figure 1. A schematic illustration showing the layout and dimension of (a) millimeter wave slot antenna and (b) tuning stub.

Table 1. Resonant frequency comparison as a function of slot dimensions.

Slot Dimensions	Resonant Frequency	Antenna Bandwidth
1.05 mm × 0.5 mm (Original)	94 GHz	> 30%
1.05 mm × 0.3 mm (Narrow)	98 GHz	28%
1.05 mm × 0.7 mm (Wide)	88 GHz	34%

Table 2. The effect of C-shaped tuning stub on antenna bandwidth performance.

Tuning Stub Inclusion	Resonant Frequency	Antenna Bandwidth
With Tuning Stub	94 GHz	> 30%
Without Tuning Stub	95 GHz	21%

shaped tuning stub used in this design helps increase the bandwidth performance of the antenna. The stub inclusion was carefully altered to not affect further integration with commercial devices. The length of the stub was 0.72 mm and width was 0.24 mm. The dimensions of the stub were optimized to achieve the maximum amount of bandwidth in the center frequency range. The width of the stub was designed equal to the width of the CPW signal line. The antenna performance was determined before and after the inclusion of tuning stub, until the element yielded maximum bandwidth and return loss. Table 2 shows a comparative result on the change in antenna bandwidth with and without a tuning stub. As noted from the table, by including the tuning stub, the resonant frequency could be centered at the desired frequency, while improving the bandwidth of the antenna to over 30%.

2.3. CPW-to-CPW Line Transition

In order to obtain the best efficiency and radiation pattern, the antenna had to be fabricated on a 10 μm silicon membrane. However, the CPW lines being fed to the antenna had to be extended beyond the thin membrane, since the membrane would undergo stress during probe test. This may potentially cause the membrane to yield, rendering the device useless. Hence, a CPW-to-CPW transition was designed in

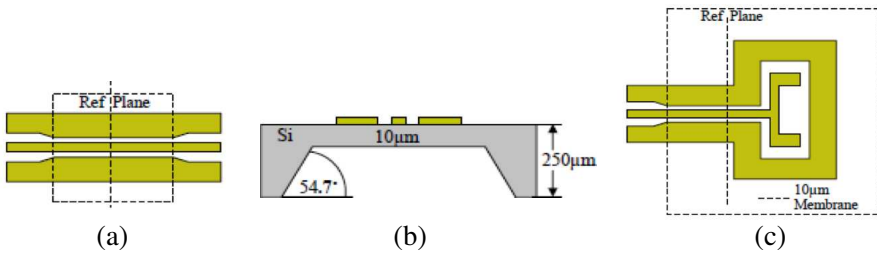


Figure 2. 94 GHz elements on a 10 μm silicon membrane. (a) CPW-to-CPW transition. (b) Silicon membrane cross-section. (c) Slot antenna.

order to probe at a thicker section of the silicon substrate, in this case, 10 μm to 250 μm transition of CPW line-width. Fig. 2 shows the layout of the line transition. The CPW slots' width decreased as the CPW line changed its thickness from 250 μm to 10 μm silicon membrane. This is the case since the dimensions of the CPW line depend on the substrate thickness. The feed line dimensions are $G = 36.5 \mu\text{m}$ and $W = 60 \mu\text{m}$ corresponding to a characteristics impedance of 50 Ω , where G is the gap between the lines and W is the width of the transmission line. The dimensions of the CPW in thinner portion of the substrate are, $G = 13.7 \mu\text{m}$ and $W = 60 \mu\text{m}$ corresponding to a characteristics impedance of 50 Ω . In order to account for the anisotropic etching of the silicon membrane, the ground planes of the CPW line were tapered as shown in Fig. 2(a) to minimize the reflections present at the discontinuity. These reflections can give birth to higher order modes, which are undesirable at the measurement's reference plane.

3. FABRICATION METHODS

The rectangular slot antennas with C-shaped tuning stub were realized on a 2'' silicon substrate. The antennas were designed to operate with a substrate thickness of 10 μm . Fig. 3 schematically illustrates the steps involved in fabricating the millimeter wave antenna. The silicon substrate was initially oxidized to form a 1 μm thick SiO_2 layer, which acts as a protective layer during backside etching. Following the oxidation of the silicon substrate, the CPW configuration pads along with the antenna were defined lithographically. The contact pads and the slot antenna structures were deposited with a thin layer of Cr and Au. Later, the membranes were patterned and chemically etched using a special set-up, described elsewhere [20]. The thickness etched was determined using a surface profilometer. Figs. 4(a) and (b) shows the SEM micrograph of the membrane-supported antenna.

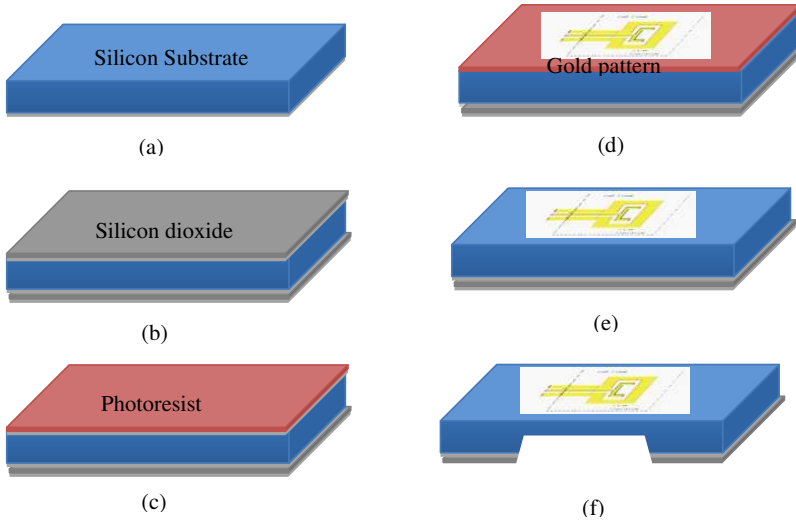


Figure 3. A Schematic of the process sequence followed to develop the slot antenna on a silicon membrane. (a) Si substrate, (b) SiO_2 grown on the substrate, (c) photoresist deposited for patterning, (d) pattern transfer by photolithography, (e) remove photoresist, (f) create a window and chemically etch the bulk silicon.

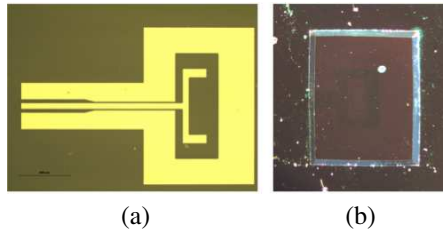


Figure 4. An optical micrograph image showing (a) the fabricated rectangular slot antenna with tuning stub and (b) a $10\ \mu\text{m}$ silicon membrane.

4. MEASUREMENT TECHNIQUES AND RESULTS

4.1. Test Set-up

The reflection coefficient measurements of the slot antennas were measured using W-band picoprobes on a Wiltron 360B network analyzer. The network analyzer was integrated with a millimeter wave expansion module (WR-10), which was capable of measuring up to

110 GHz. Waveguide probes with $150\ \mu\text{m}$ pitch were used to measure the antenna parameters at millimeter wave frequency. TRL calibration was used to move the reference plane from the probe tip to the plane shown in Fig. 2.

4.2. Measurement

The simulated and measured reflection co-efficient of rectangular slot antenna is illustrated in Fig. 5. It can be seen that the antenna presents well-matched input impedance at the design frequency. However, there is a slight frequency shift between the measured and simulated results, which could be due to the variations in the thickness of the membrane. A return loss of $-35.7\ \text{dB}$ at $93.6\ \text{GHz}$ with a $-10\ \text{dB}$ bandwidth of over 30% has been measured for the $94\ \text{GHz}$ antenna. The simulated response indicates over 28% bandwidth at $-10\ \text{dB}$, which agrees well with the measured response.

Additionally, to validate the ultra wideband response of the antenna, several antennas were fabricated with the same dimensions and tested. Fig. 6 illustrates the results for the other antennas. It can be observed that all the antennas fall within the design frequency range. The return loss was found to be varying from $-26\ \text{dB}$ to $-35\ \text{dB}$, while resonating from $93.6\ \text{GHz}$ to $96.5\ \text{GHz}$. This variation in frequency response has been determined to be the variation in the substrate thicknesses. Nevertheless, all the antennas demonstrated almost similar bandwidth, as shown in Fig. 6, validating the inclusion of the tuning stub improves the bandwidth of a conventional slot antenna.

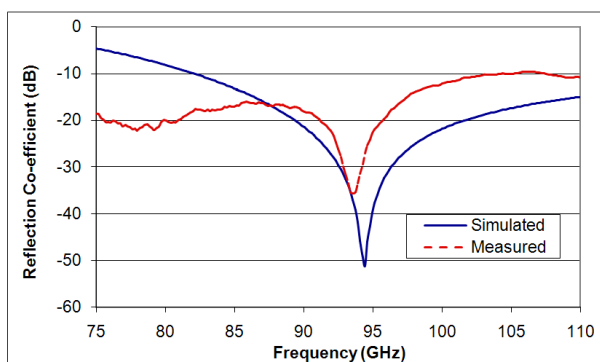


Figure 5. Measured vs. simulated antenna return loss of the $94\ \text{GHz}$ slot antenna with tuning stub.

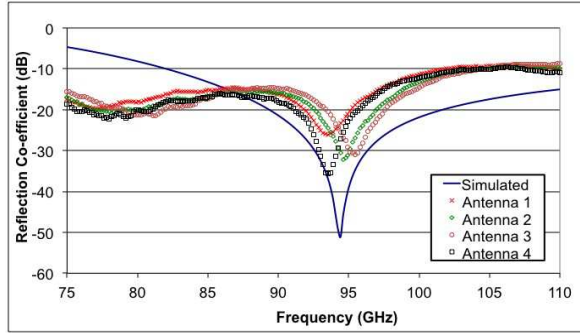


Figure 6. Measured vs. simulated antenna return loss of the different slot antennas.

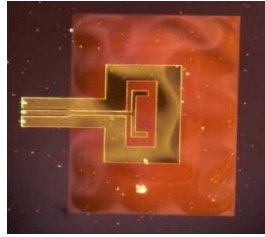


Figure 7. An optical micrograph of a slot antenna fabricated on an over-etched silicon membrane.

4.3. Effect of Varying Membrane Thickness

Based on the previous experiment, a control experiment was also devised. In this experiment, the thickness of the membrane was etched to $1\ \mu\text{m}$ and the antenna response was determined. The thickness of the membrane was verified using a surface profilometer. An optical micrograph of an over-etched silicon membrane with slot antenna is shown in Fig. 7. It can be observed that the silicon membranes in Fig. 7 are more transparent than those presented in Fig. 4. The transparency of the membranes is an indication of the membrane thickness. The electrical measurement of these antennas was also done using the earlier mentioned set-up. A comparison between the simulated and measured slot antennas is presented in Fig. 8.

This change in membrane definition had an immediate effect on the measured antenna results. The noticeable frequency shift in Fig. 8 clarifies the above-mentioned problem that can arise when the substrate membrane is over etched. It is also observed that, the variation in substrate thickness can also give rise to resonant frequencies to appear in a non-ordered manner.

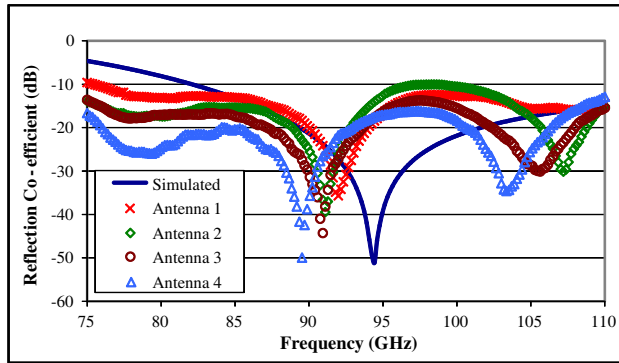


Figure 8. Measured vs. simulated antenna return loss of the different slot antennas on over-etched membrane.

4.4. Analysis of Radiation Pattern

The radiation pattern of the antenna was simulated in ADS, as shown in Fig. 9. The coordinate system and the position of the antenna are represented in the schematic along with the current distribution of the slot. The maximum co-polarization magnitude achieved was -3 dB at 0° with a gain of 4.5 dBi. Table 3 below demonstrates the variation of gain with respect to frequency in the resonating band. The antenna demonstrated an omnidirectional radiation pattern by achieving maximum radiation at right angles to the dipole and then dropping off to zero on the antenna’s axis.

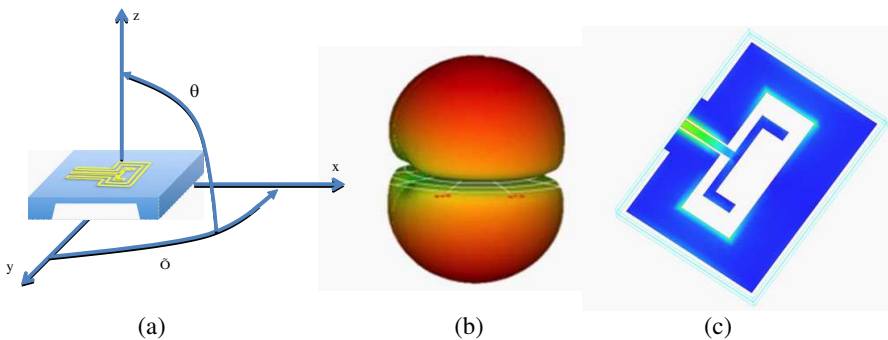


Figure 9. Simulated Co-Polarized radiation pattern (dB) of the wideband millimeter antenna showing (a) the coordinate system and the position of the antenna, (b) the 3D radiation pattern, and (c) the current distribution of the slot antenna.

Table 3. Variation of gain in the resonating band.

Resonant Frequency	Gain (dBi)
60 GHz	4.05
64 GHz	4.1
68 GHz	4.15
72.5 GHz	4.19
76 GHz	4.25
94 GHz	4.5
110 GHz	4.87

5. CONCLUSION

A millimeter wave wideband slot antenna with a C-shaped tuning stub, fabricated on a silicon membrane was presented. Through parametric studies, momentum results indicate that in millimeter wave frequencies, thicker substrates create more surface wave propagation presenting dominating side lobes, distorting the overall radiation pattern of the antenna. Simulation results indicate that the best reflection coefficient of the antenna was achieved with a substrate thickness of $10\ \mu\text{m}$. All the fabricated antennas provided reflection coefficient of $-10\ \text{dB}$ or greater. The antenna also achieved a bandwidth of 30% referenced to a reflection coefficient $\geq 10\ \text{dB}$ when a tuning stub was introduced in the slot antenna. Results also indicate that antenna gain increases as the resonant frequency increases.

ACKNOWLEDGMENT

The authors are grateful for the funding support provided by the State of Florida through the Florida Energy Systems Consortium (FESC) funds. The authors would like to acknowledge the Nanotechnology Research and Education Center (NREC) and the Wireless and Microwave Center (WAMI) for providing the fabrication and measurement facility.

REFERENCES

1. Yeom, S., D. Lee, H. Lee, J. Son, and V. P. Gushin, "Distance estimation of concealed objects with stereoscopic passive millimeter-wave imaging," *Progress In Electromagnetics Research*, Vol. 115, 399–407, 2011.

2. Zhang, J.-C., Y.-Z. Yin, and J.-P. Ma, "Design of narrow band-pass frequency selective surfaces for millimeter wave applications," *Progress In Electromagnetics Research*, Vol. 96, 287–298, 2009.
3. Mohammad-Taheri, M., M. Fahimnia, Y. Wang, M. Yu, and S. Safavi-Naeini, "Wave analysis for inductively matched millimeter wave amplifier design," *Progress In Electromagnetics Research C*, Vol. 13, 41–50, 2010.
4. Ali-Ahmad, W. Y., G. V. Eleftheriades, L. P. B. Katehi, and G. M. Rebeiz, "Millimeter-wave integrated-horn antenna. II. Experiment," *IEEE Transactions on Antennas and Propagation*, Vol. 39, No. 11, 1582–1586, Nov. 1991.
5. Cogdell, J., J. J. McCue, P. Kalachev, A. Salomonovich, I. Moiseev, J. Stacey, E. Epstein, E. Altshuler, G. Feix, J. Day, H. Hvatum, W. Welch, and F. Barath, "High resolution millimeter reflector antennas," *IEEE Transactions on Antennas and Propagation*, Vol. 18, No. 4, 515–529, Jul. 1970.
6. Sekelsky, S. M. and J. Carswell, "High power electronic scanning millimeter-wave radar system design," *IEEE Aerospace Conference*, Jul. 24, 2006.
7. Deng, K. L., C. C. Meng, S. S. Lu, H. D. Lee, and H. Wang, "A fully monolithic integrated twin dipole antenna mixer on a GaAs substrate," *Asia-Pacific Microwave Conference*, Aug. 6, 2002.
8. Manasson, V. A. and L. S. Sadovnik, "Monolithic electronically controlled millimeter-wave beam steering antenna," *1998 Topical Meeting on Silicon Monolithic Integrated Circuits in RF systems*, Aug. 6, 2002.
9. Hirokawa, J., M. Zhang, and M. Ando, "94 GHz fabrication of a slotted waveguide array antenna by diffusion bonding of laminated thin plates," *IEEE Sensors*, 907–911, Oct. 2009.
10. Najafi, K., "Recent progress in micromachining technology and application in implantable biomedical systems," *Sixth International Symposium on Micro Machine and Human Science*, 11–20, Aug. 6, 2002.
11. Gauthier, G. P., J.-P. Raskin, L. P. B. Katehi, and G. M. Rebeiz, "A 94-GHz aperture-coupled micromachined microstrip antenna," *IEEE Transactions on Antennas and Propagation*, Vol. 47, No. 12, 1761–1766, Dec. 1999.
12. Felic, G. and E. Skafidas, "A CPW-fed loop slot antenna for integration with millimeter wave CMOS transceiver," *European Wireless Technology Conference*, 77–80, Oct. 23, 2009.

13. Bhohe, A. U., C. L. Holloway, M. Piket-May, and R. Hall, "Wideband slot antennas with CPW feed lines: Hybrid and log-periodic design," *IEEE Transactions on Antennas and Propagation*, Vol. 52, No. 10, 2545–2554, Oct. 2004.
14. Nedil, M., L. Talbi, and T. A. Denidni, "Design of broadband printed slot antennas for wireless millimeter-wave applications," *Topical Conference on Wireless Communication Technology*, 23–24, Aug. 24, 2004.
15. Raman, S., T. M. Weller, L. P. B. Katchi, and G. M. Rebeiz, "A double folded-slot antenna at 94 GHz," *Antennas and Propagation Society International Symposium, AP-S. Digest*, Vol. 1, 710–713, Jun. 18–23, 1995.
16. Kobayashi, H. and Y. Yasuoka, "Slot-array antennas fed by coplanar waveguide for millimeter-wave radiation," *IEEE Transactions on Microwave Theory and Techniques*, Vol. 46, No. 6, 800–805, Jun. 1998.
17. Ellis, T. J., J.-P. Raskin, G. M. Rebeiz, and L. P. Katehi, "A wideband CPW-fed microstrip antenna at millimeter-wave frequencies," *IEEE Antennas and Propagation Society International Symposium*, Vol. 2, 1220–1223, Aug. 1999.
18. Elazar, G. and M. Kisiuk, "Microstrip linear slot array antenna for X-band," *IEEE Transactions on Antennas and Propagation*, Vol. 36, No. 8, Aug. 1998.
19. Saed, M. A., "Broadband CPW-FED planar slot antennas with various tuning stubs," *Progress In Electromagnetics Research*, Vol. 66, 199–212, 2006.
20. Krishnan, S., "Thin film metal-insulator-metal tunnel junctions for millimeter wave detection," *Theses and Dissertations*, Paper 346, 2008.